

N.K. Tanasheva, M.A. Burkov, A.N. Dyusembayeva, S. Suleimenova, A.S. Tussupbaeva,
Sh.S. Kyzdarbekova

Karaganda University of the name of academician E.A. Buketov, Kazakhstan
(*E-mail: maxim19990202@gmail.com)

Determination of the optimal deflection angle of the sail blade of a wind power plant

This article presents the results of studies of a sailing wind power plant at various parameters. For this purpose, a model of a wind power plant controlled by a system of sail blades was developed. Studies of aerodynamic forces at different angles of deflection of the sail blade system were carried out: 0°; 30°; 60°; 90°. The air flow velocity varied in the range from 3 to 14 m/s. The experiments were carried out in a T-1-M wind tunnel designed to measure forces and moments acting on a sailing wind turbine. As a result of experiments, it was found that with an increase in the air flow velocity, the frequency of rotation of the shaft of the wind power plant increased. The maximum rotational speed of the shaft was reached at $\alpha = 0^\circ$ deflection of the sail blade system of the wind power plant. A number of experiments were carried out and aerodynamic characteristics were obtained depending on the deflection angle (α) of the sail blade system of the wind power plant and the air flow velocity. As the deflection angle of the blade system increases, the drag force decreases depending on the air flow velocity. It was experimentally established that at $\alpha = 30^\circ$ deflection of the blade system created the maximum lift force. Based on the data obtained, it was found that with an increase in the speed of the incoming air flow, the aerodynamic forces acting on the sailing wind power plant increased.

Keywords: Sail blade, wind power plant, shaft rotation speed, wind turbine, deflection angle, frontal resistance, thrust force, T-1-M wind tunnel.

Introduction

Due to its geographical features, Kazakhstan has high potential for wind energy, which can be harnessed to generate electricity and reduce dependence on oil and gas resources. In recent years, Kazakhstan has been actively developing wind energy, attracting foreign investment and building new wind farms, to achieve energy independence and reduce greenhouse gas emissions. The average wind speed reaches 3-4 m/s in most of the territory, while in open areas, the air flow velocity is 6 m/s or higher [1].

When analyzing wind energy technologies, it is evident that the most common type is wind generators with blade rotors used in turbine wind power plants. However, these installations face challenges related to the unpredictability of wind speed and direction, as well as limited operating speed range, making them less effective in Kazakhstan [2]. Traditional bladed wind power plants also have low efficiency at low wind speeds, particularly in the repetitive wind range of 6-7 meters per second [3, 4]. To address this issue, a sailing wind power plant is being used.

One advantage of a sailing wind power plant is its ability to generate electrical energy from low wind speeds, as low as 3 m/s [5]. The wind turbine operates by utilizing the kinetic energy of the wind, converting it into mechanical energy through the rotation of the shaft with the help of torque resulting from the aerodynamic lift force on the sails. However, existing sailing wind power plants lack a mechanism to regulate the deflection angle of the blades.

The novelty of this installation lies in the use of a controlled system of blades, which provides optimal conditions for operation [6]. By adjusting the deflection angle of the sail blades, the load on the wind power plant can be reduced during high wind speeds. The objective of this study is to investigate the aerodynamic characteristics of a sailing wind power plant using a controlled system of blades in the form of a triangular sail, calculate the drag and thrust coefficients, determine the optimal deflection angle of the blades, and demonstrate the effectiveness of this wind power plant.

Experimental

In this study, experiments were conducted using a mock-up of an eight-bladed sailing wind power plant to investigate the effect of flow direction on its aerodynamic characteristics.

An experimental model of an eight-bladed sailing wind power plant was created for the purpose of research. Aerodynamic characteristics were measured at least five times. The wind power wheel had a diameter of $d = 0.43$ [m], the cross-sectional diameter of the model was $S = 0.145$ [m], the area covered by the rotor was $R = 0.215$ [m], the air density was $\rho = 1.21$, and the kinematic viscosity of the air was $\nu = 14.9 \cdot 10^{-5}$ [Pa·s]. The measurement error was within 4 %.

The experiments were conducted in the working section of the T-1-M wind tunnel, which had a diameter of the working part $D = 0.5$ m and a length $L = 0.8$ m. Drag force measurements were carried out using three-component aerodynamic scales with high measurement accuracy. Figure 1 shows a diagram of the experimental eight-blade sailing wind power plant.

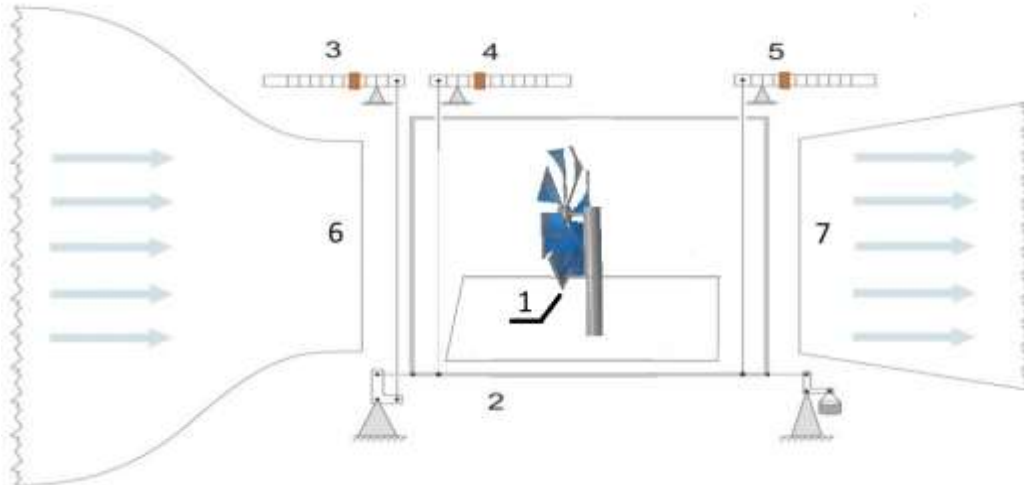


Figure 1. Diagram of an experimental sailing wind turbine

1 — Sailing blades of a wind power plant; 2 — a frame for mounting a mock-up with aerodynamic scales; 3 — scales measuring drag force; 4 — scales measuring lift; 5 — confuser; 6 — wind tunnel diffuser [7].

The angle of deflection of the blades is an important parameter for the energy efficiency of the wind turbine, as it affects the direction and speed of the air flow passing through the turbine. In Figure 2, the angle of deflection of the sail was varied to the following values: 0° , 15° , 30° , 45° , and 60° .

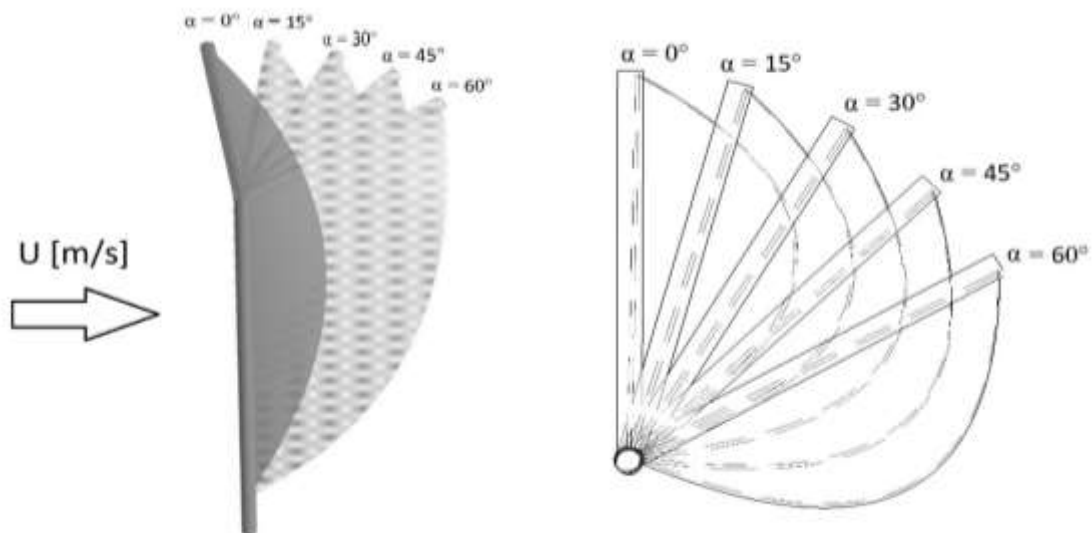


Figure 2. Changes in the deflection angle (α) of the blades of a sailing wind power plant.

During the experiments, a decrease in efficiency was observed at flow installation angles exceeding $\alpha = 60^\circ$. Experiments were not conducted at angles α greater than 60° .

The following formula (1) was used to determine the drag coefficient (C_x), thrust coefficient, and Reynolds number (Re):

$$C_x = \frac{F_x}{\rho \cdot \frac{u^2}{2} \cdot S}, C_m = \frac{F_m}{\rho \cdot \frac{u^2}{2} \cdot S}, Re = \frac{u \cdot d}{\nu} \quad (1)$$

where F_x is the drag force [N], F_t is the thrust force [N], ρ is the air density [kg/m^3], u is the air flow velocity [m/s], S is the midsection area of the rotor [m^2], d is the diameter [m], and ν is the kinematic viscosity of the air [m^2/s] [8].

During the experiments, the air flow velocity varied from 3 m/s to 14 m/s. The number of revolutions was measured using a digital laser photo tachometer AT-8, and the velocity of the incoming air flow was measured using a Skywatch Atmos cup anemometer [9-10].

Results and Discussion

Based on experimental data (Fig. 3), the dependence of the number of rotations of the shaft of a sailing wind turbine (N) on the wind speed (U) and the angle of deflection of the sailing blades (α) is obtained.

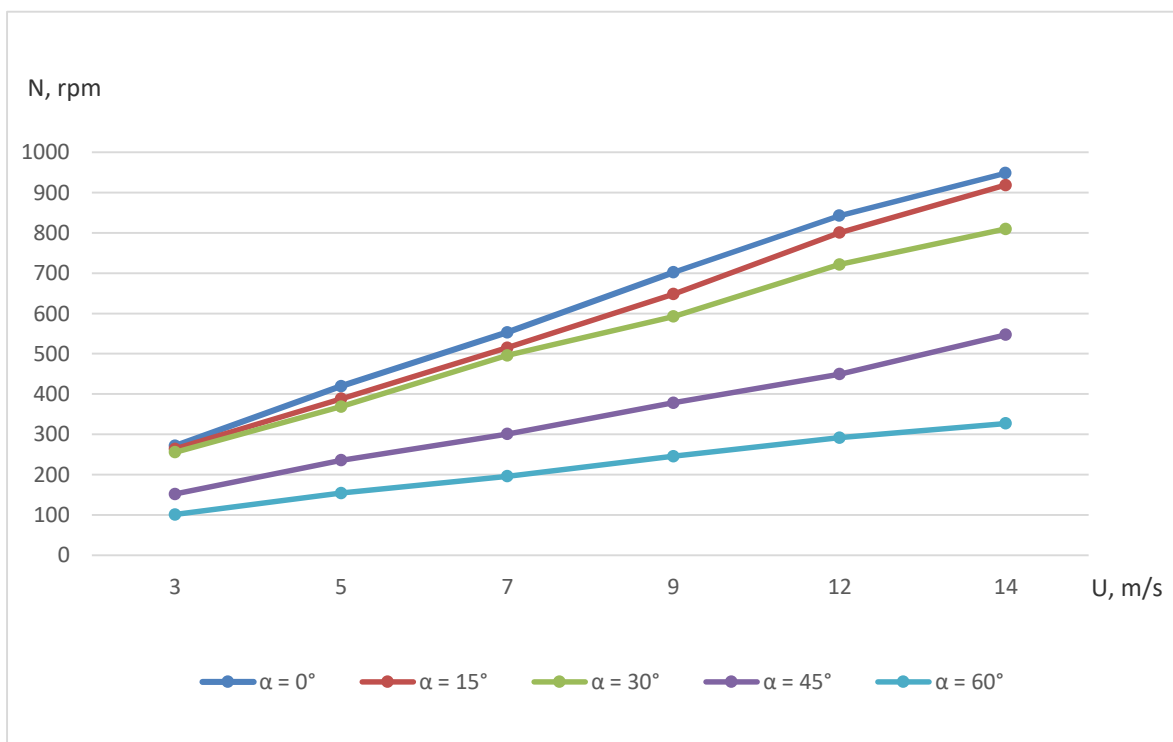


Figure 3. The dependence of the number of revolutions (N) of a sailing wind power plant on the wind speed (U) and the angle of deflection of the sailing blades (α).

From the data obtained, the maximum value of the drag force of a sailing wind power plant is reached at $\alpha=0^\circ$, with a rotational speed of $n=271$ [rpm] at $U=3$ m/s, and gradually increases (from 4 m/s to 14 m/s) depending on the air flow velocity ($n=948$ [rpm], $U=14$ m/s). With a change in the angle of deflection of the sailing blades, the number of revolutions rapidly decreases. The minimum rotation speed of the wind turbine shaft is $n=195$ [rpm] at $\alpha=60^\circ$ and $U=3$ m/s, and $n=326$ [rpm] at $U=14$ m/s.

The rise in wind speed leads to a smooth increase in the dynamic air pressure on the soul blade of the wind power plant, which contributes to its acceleration. Further experiments were carried out to measure the drag force (F_d). Figure 4 describes the dependence of the drag force (F_d) of a sailing wind power plant on the wind speed (U) at different angles of deflection of the sailing blades (α).

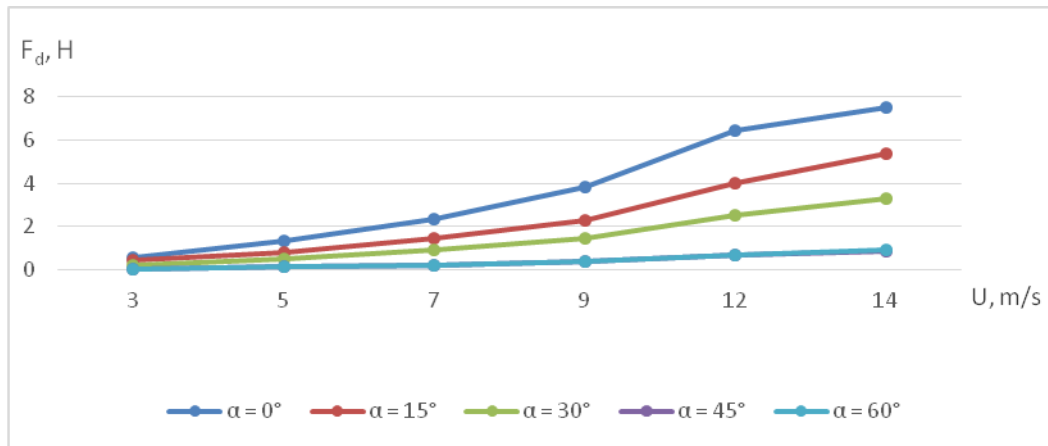


Figure 4. Dependence of the drag force (F_d) of a sailing wind power plant on wind speed at different angles of deflection of the sailing blades (α).

With a minimum deflection angle $\alpha = 0^\circ$ (Fig. 4), the maximum drag force $F_d = 0.575\text{ N}$ (for $U = 3\text{ m/s}$) is observed, and it gradually rises with higher wind speeds, reaching $F_t = 7.506\text{ N}$ at $U = 14\text{ m/s}$. When the deflection angle of the blades changes, the drag force ($\alpha = 15^\circ - 60^\circ$) decreases rapidly, reaching $F_t = 26\text{ N}$ at $\alpha = 15^\circ$ and $U = 3\text{ m/s}$, and gradually climbs with higher air flow velocities, reaching $F_t = 0.911\text{ N}$ at $\alpha = 60^\circ$ and $U = 14\text{ m/s}$. As the air flow velocity increases, the dynamic pressure effect leads to an augmentation in the drag force on the surface of the blades. Consequently, with a minimum angle of deflection of the blade ($\alpha = 0^\circ$), the flow passes more smoothly and with minimal energy losses, allowing for maximum frontal pressure on the surface of the blade. Further studies were carried out to measure the thrust force of a sailing wind power plant as a function of the air flow velocity (Fig. 5).

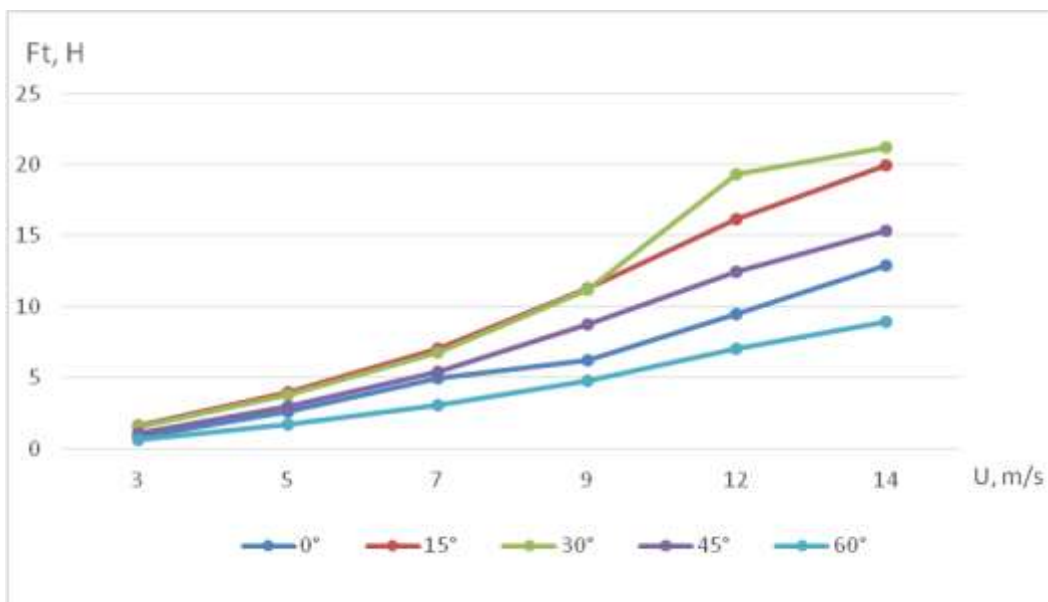


Figure 5 The thrust force (F_t) of a sailing wind power plant as a function of the air flow velocity (U)

As can be seen from Figure 5, the thrust force (F_t) on the sail blades depends on the deflection angle (α) of the air flow. At small deflection angles ($\alpha = 0^\circ - 30^\circ$), the air flow is almost parallel to the surface of the blades, which creates a large thrust force. Consequently, at $\alpha = 0^\circ$, the thrust force is $F_t = 0.81\text{ N}$ (at $U = 3\text{ m/s}$) and $F_t = 12.9\text{ N}$ (at $U = 14\text{ m/s}$). When the angle of the sail blades changes, the part of the kinetic energy of the wind is converted into the potential energy of the sail. The sail begins to work like a wing, creating not only horizontal thrust, but also vertical lift. Consequently, at $\alpha = 30^\circ$ deflection of the blades, the thrust force has a maximum value of $F_t = 1.6\text{ N}$ (at $U = 3\text{ m/s}$) and reaches ($F_t = 19.99\text{ N}$ at $U = 14\text{ m/s}$.)

Thus, at large deflection angles (more than $\alpha = 30^\circ$), the air flow begins to break and form vortices behind the blades ($\alpha = 45^\circ F_t=1.56$ at $U=3$ m/s) and ($F_t= 21.25$ N at $U=14$ m/s), which leads to a smooth decrease in the thrust force ($\alpha = 60^\circ F_t=0.7$ N at $U=3$ m/s and ($F_t= 8.96$ at $U=14$ m/s).

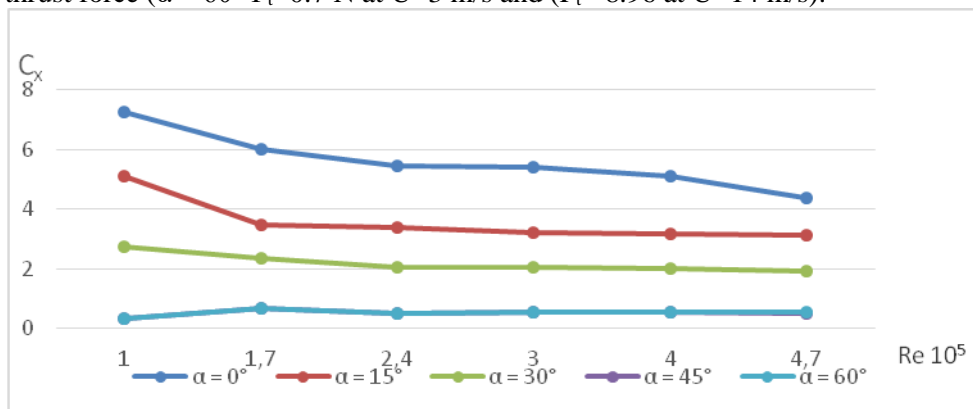


Figure 6. Dependence of the drag coefficient on the Reynolds number for a sailing wind power plant at different angles of deflection of the sailing blades

As the Reynolds number increases (Fig. 6), the pressure on the surface of the sail blades gradually rises. This phenomenon leads to a decrease in the frontal coefficient at $\alpha = 0^\circ C_x = 0.73$ (at $Re = 10^5$) and $C_x = 0.44$ (at $Re= 4.7 \cdot 10^5$).

When the deflection angle changes, the vector of the force acting on the sail blades changes. As a result, the resistance force also changes, which is displayed on the charts depending on the angle of deviation in the range: $\alpha =$ from 0 to 60° . At a deflection angle $\alpha = 60^\circ$ ($C_x = 0.0329$ at $Re = 10^5$) and ($C_x = 0.077$ at $4.7 \cdot 10^5$).

Thus, the changes in the drag coefficients on the graph are due to changes in the Reynolds number and the deflection angle of the sail blades.

Figure 7 shows the dependence of the thrust coefficient (C_t) on the Reynolds number (Re) for a sailing wind power plant.

The studies were carried out at different angles of deflection of the blades (from $\alpha = 0^\circ$ to 60°) for this wind power plant.

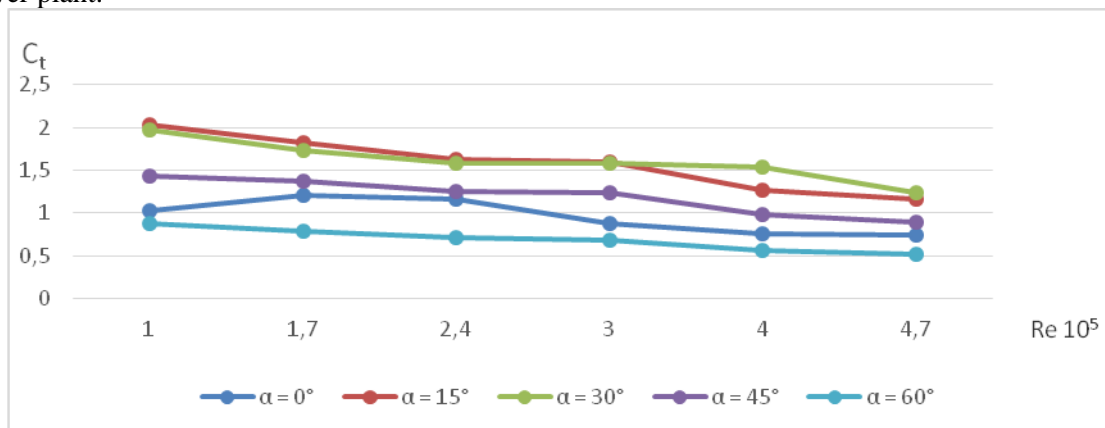


Figure 7. Dependence of the thrust coefficient on the Reynolds number for a sailing wind power plant

With an increase in the Reynolds number (Fig. 7), the thrust coefficient grows and reaches a maximum at the angle of deflection of the blades $\alpha = 30^\circ C_t = 2$ (at $Re = 10^5$) and $C_t = 1.16$ (at $Re = 4.7 \cdot 10^5$), then decrease with a further increase in the angle of attack. This is due to changes in the flow conditions of the installation surface at different wind speeds and deflection angles of the blades.

Conclusions

Based on the results obtained, the following conclusions can be drawn:

- an experimental model with the specified parameters was developed, which was subsequently carried out experimental studies in the T-1-M wind tunnel in order to obtain data on aerodynamic characteristics.

- the number of rotations of the shaft of the wind power plant from the air flow velocity is set. The maximum rotation speed of the wind turbine shaft is fixed at $N = 948$ [rpm] at $U = 14$ m/s. A high number of revolutions leads to excessive wear and damage to the equipment, as well as to an excess of noise and vibrations. The data obtained will help to choose the angle of deflection of the sail blades for optimal operation of the wind power plant.

- the dependence of the drag force on the air flow velocity is obtained. It is established that with an increase in the air flow velocity, the drag force rises smoothly. The maximum drag force was reached at $U = 14$ m/s ($F_d = 0.911$ N).

Experimental data showed that in order to obtain the maximum thrust force, it is necessary to select the optimal angle of deflection of the blades, in our case, with a deflection angle $\alpha = 30^\circ$ of peak values, the thrust force reached $F_t = 1.607$ N ($U = 14$ m/s).

- the optimal deflection angle $\alpha = 30^\circ$ is determined, where the maximum coefficient of thrust of the sail blades ($C_t = 2$) is fixed (Reynolds number $1,7 \cdot 10^5$). With a slight deflection of the blades, the wind acts on the blades at a certain angle, creating a lifting force that leads to the rotation of the rotor of the wind turbine and an increase in the thrust force. However, as the deflection angle of the sail blades increases, the lifting force reaches its maximum and begins to decrease, as the wind ceases to affect the blades at the same angle. This leads to a decrease in the thrust force on the blades, which in turn leads to a slowdown in the rotation of the wind turbine rotor.

Thus, the data obtained will make it possible to create and develop a wind energy system. An installation that will allow rational and efficient use of wind energy resources. Also, with the help of a controlled system of blades, you can choose the optimal angle of deviation for more productive use of the wind power plant.

Acknowledgment

The work was carried out with the financial support of the Science Committee of the Ministry of Science and Higher Education of the Republic of Kazakhstan (IRN AP14870066 “Development and creation of an energy-efficient combined vertical-axial wind power plant using a gearless low-speed electric generator”).

References

- 1 Глеубергенова А.Ж. Исследование аэродинамических сил треугольной лопасти ветротурбины при низких скоростях ветра / А.Ж. Глеубергенова, Н.К. Танашева, К.М. Шаймерденова, Л.Л. Миньков, С.Ж. Узбергенова // Eurasian Physical Technical Journal. — 2021. — Т. 18, № 4 (38). — С. 59–64.
- 2 Алибекова А.Р. Экспериментальные испытания опытной ветроэнергетической установки в условиях естественного ветра при различных климатических условиях // А.Р. Алибекова, К.К. Кусаиынов, Ж.Т. Камбарова, Н.К. Танашева, М.Б. Карагаева // Вестн. Караганд. ун-та. Сер. Физика. — 2015. — № 2 (78). — С. 44–49.
- 3 Танашева Н.К. Исследование зависимости аэродинамических характеристик вращающихся цилиндров от угла скоса воздушного потока / Н.К. Танашева, Н.Н. Шуюшбаева, Н.К. Мусенова // Письма в ЖТФ. — 2018. — Т. 44, № 17. — С. 63–65.
- 4 Han J-B. An aerodynamic model for insect flapping wings in forward flight / J-B. Han, J.W. Chang, J-H. Han // Journal of Bioinspiration and Biomimetics. — 2017. — Vol. 12. — P. 3600–36014
- 5 Noest R.M. Optimal wing hinge position for fast ascent in a model fly / R.M. Noest, Z.J. Wang // Journal of Fluid Mechanics — 2018. — Vol. 849. — P. 498-509.
- 6 Hosseinie R. Parametric study of a novel oscillatory wind turbine / R. Hosseinie, R. Roohi, G Ahmadi // Journal of Energy Equipment and Systems — 2018. — Vol. 7, No. 4 — P. 377 — 387
- 7 Hosseinie R. Parametric study and performance analysis of a swinging sail wind machine / R. Hosseinie, R. Roohi, G. Ahmadi // Journal of Energy Conversion and Management. — 2020. — Vol. 205 — P. 112452—112465
- 8 Wang Z.J. Insect flight: from Newton's law to neurons / Z.J. Wang // Annual Review of Condensed Matter Physics. — 2016. — Vol. 7. — P. 281—300.
- 9 Kumar A. Performance analysis of a Savonius hydrokinetic turbine having twisted blades. / A. Kumar, R.P. Saini // Journal of Renewable Energy. — 2017. — Vol. 108. — P. 502—522.
- 10 Kumar A. Performance analysis of a single stage modified Savonius hydrokinetic turbine having twisted blades / A. Kumar, R.P. Saini // Journal of Renewable Energy. — 2017. — Vol. 113. — P. 461—478.

Н.К. Танашева, М.А. Бурков, А.Н. Дюсембаева, С. Сулейменова, А.С. Тусупбаева,
С.С. Кыздарбекова

Жел энергетикалық қондырғының желкенді қалақшасының оңтайлы ауытқу бұрышын анықтау

Мақалада желкенді жел қондырғысын әртүрлі параметрлерде зерттеу нәтижелері келтірілген. Осы мақсатта басқарылатын қалақ жүйесі бар жел қондырғысының макеті жасалды. Желкенді қалақшаның ауытқуының әртүрлі бұрыштарындағы аэродинамикалық күштерге зерттеулер жүргізілді: 0° ; 30° ; 60° ; 90° . Тәжірибелер желкенді жел турбинасына әсер ететін күштер мен моменттерді өлшеуге арналған Т-1-М жел туннелінде жүргізілді. Жүргізілген тәжірибелер нәтижесінде ауа ағынының жылдамдығы артқан сайын жел электр станциясының білігінің айналу жиілігі артатыны анықталды. Біліктің максималды айналу жиілігіне жел қондырғысының желкенді қалақтары $\alpha = 0^\circ$ ауытқыған кезде қол жеткізіледі. Жел электр станциясының желкенді қалақтарының ауытқу бұрышына (α) және ауа ағынының айналу жылдамдығына байланысты бірқатар эксперименттер жүргізіліп, аэродинамикалық сипаттамалар алынды. Тәжірибе барысында қалақшаның ауытқу бұрышы артқан кезде ауа ағынының жылдамдығына байланысты кедергі күші азаятыны анықталды. $\alpha = 30^\circ$ кезінде желкенді қалақшалардың ауытқуы максималды тарту күшін тудыратыны тәжірибе негізінде дәлелденді. Алынған мәліметтер негізінде аэродинамикалық коэффициенттердің өзгеру графиктері (фронтальды кедергі, жел электр станциясының тартылуы) ұсынылған. Қарсы ауа ағынының жылдамдығының жоғарылауымен желкенді жел қондырғысына әсер ететін аэродинамикалық күштер көбейетіні анықталды. Бұл зерттеудің нәтижелері басқарылатын қалақша жүйесі бар желкенді жел қондырғыларын одан әрі дамыту үшін пайдалы болуы және жел энергиясын өндіруде осындай жүйелердің тиімділігін арттыруға ықпал етуі мүмкін.

Кілт сөздер: желкенді қалақша, жел энергетикалық қондырғы, біліктің айналу жиілігі, жел турбинасы, ауытқу бұрышы, маңдай кедергі, тарту күші, Т-1-маэродинамикалық құбыр.

Н.К. Танашева, М.А. Бурков, А.Н. Дюсембаева, С. Сулейменова, А.С. Тусупбаева,
Ш.С. Кыздарбекова

Определение оптимального угла отклонения парусной лопасти ветроэнергетической установки

В статье приведены результаты исследований парусной ветроэнергетической установки при различных параметрах. Для данной цели разработан макет ветроэнергетической установки, управляемой системой лопастей. Проведены исследования аэродинамических сил при различных углах отклонения парусных лопастей: 0° ; 30° ; 60° ; 90° . Скорость воздушного потока варьировалась в диапазоне от 3 до 14 м/с. Эксперименты проводились в аэродинамической трубе Т-1-М, предназначенной для измерений сил и моментов, действующих на парусную ветротурбину. В результате проведенных экспериментов установлено, что с увеличением скорости воздушного потока возрастает частота вращения вала ветроэнергетической установки. Максимальная частота вращения вала достигается при $\alpha=0^\circ$ отклонения парусных лопастей ветроэнергетической установки. Проведен ряд экспериментов и получены аэродинамические характеристики в зависимости от угла отклонения (α) парусных лопастей ветроэнергетической установки и скорости обтекания воздушным потоком. В ходе проведения экспериментов установлено, что при увеличении угла отклонения лопасти сила лобового сопротивления уменьшается в зависимости от скорости воздушного потока. Экспериментально доказано, что при $\alpha=30^\circ$ отклонения парусных лопастей создается максимальная сила тяги. На основе полученных данных представлены графики изменения аэродинамических коэффициентов (лобового сопротивления, тяги ветроэнергетической установки). Определено, что с увеличением скорости набегающего потока воздуха аэродинамические силы, действующие на парусную ветроэнергетическую установку, возрастают.

Ключевые слова: парусная лопасть, ветроэнергетическая установка, частота вращения вала, ветротурбина, угол отклонения, лобовое сопротивление, сила тяги, аэродинамическая труба Т-1-М.

References

- 1 Pleubergenova, A.Zh., Tanasheva, N.K., Shaimerdenova, K.M., Minkov, L.L. & Uzbergenova, S.Zh. (2021). Issledovanie aerodinamicheskikh sil treugolnoi lopasti vetroturbiny pri nizkikh skorostiakh vetra [Investigation of the aerodynamic forces of a triangular wind turbine blade for the low wind]. *Eurasian Physical Technical Journal*, 18, 4(38), 59–64 [in Russian].

- 2 Alibekova, A.R., Kusainov, K.K., Kambarova, Z.T., Tanasheva, N.K. & Karagaeva, M.B. (2015). Eksperimentalnye ispytaniia opytnoi vetroenergeticheskoi ustanovki pri razlichnykh klimaticheskikh usloviakh [Experimental tests of an experimental wind power plant in natural wind under different climatic conditions]. *Vestnik Karagandinskogo universiteta. Seriya Fizika — Bulletin of the Karaganda University. Physics series*, 2(78), 44–49 [in Russian].
 - 3 Tanasheva, N.K., Shuyushbaeva, N.N. & Musenova, N.K. (2018). Issledovanie zavisimosti aerodinamicheskikh kharakteristik vrashchaiushchikhsia tsilindrov ot ugla skosa vozdušnogo potoka [Investigation of the dependence of the aerodynamic characteristics of rotating cylinders on the angle of the bevel of the air flow]. *Pisma v ZhTF — Letters to the Journal of Technical Physics*, 44, 17, 63–65 [in Russian].
 - 4 Han, J-B., Chang, J.W. & Han, J-H. (2017). An aerodynamic model for insect flapping wings in forward flight. *Journal of Bioinspiration and Biomimetics*, 12, 3600–36014.
 - 5 Noest, R.M. & Wang, Z.J. (2018). Optimal wing hinge position for fast ascent in a model fly. *Journal of Fluid Mechanics*. 849, 498–509.
 - 6 Hosseinie R., Roohi R. & Ahmadi, G. (2018). Parametric study of a novel oscillatory wind turbine. *Journal of Energy Equipment and Systems*, 7(4), 377–387
 - 7 Hosseinie, R., Roohi, R. & Ahmadi, G. (2020). Parametric study and performance analysis of a swinging sail wind machine. *Journal of Energy Conversion and Management*, 205, 112452—112465
 - 8 Wang, Z.J. (2016). Insect flight: from Newton's law to neurons. *Annual Review of Condensed Matter Physics*, 7, 281—300.
 - 9 Kumar, A. & Saini, R.P. (2017). Performance analysis of a Savonius hydrokinetic turbine having twisted blades. *Journal of Renewable Energy*, 108, 502—522.
- Kumar, A. & Saini, R.P. (2017). Performance analysis of a single stage modified Savonius hydrokinetic turbine having twisted blades. *Journal of Renewable Energy*, 113, 461—478.